Title

Systematic evaluation of Copper(II)-loaded immobilized metal affinity chromatography for selective enrichment of copper-binding species in human serum and plasma

Journal

Metallomics, 14(9)

ISSN

1756-5901

Authors

Janisse, Samuel E

Sharma, Vibha A

Caceres, Amanda

et al.

Publication Date

2022-09-01

DOI

10.1093/mtomcs/mfac059

Peer reviewed

Metallomics, 14, 2022, mfac059
https://doi.org/10.1093/mtomcs/mfac059
Advance access publication date: 5 August 2022
Paper

Systematic evaluation of Copper(II)-loaded immobilized metal affinity chromatography for selective enrichment of copper-binding species in human serum and plasma

Samuel E. Janisse [1], Vibha A. Sharma[1], Amanda Caceres[1], Valentina Medici [2] and Marie C. Heffern [1,*]

[1]Department of Chemistry, University of California Davis, Davis, CA 95616, USA and [2]Department of Internal Medicine, Division of Gastroenterology and Hepatology, University of California Davis, Sacramento, CA 95817, USA
*Correspondence: Marie C. Heffern, Department of Chemistry, University of California Davis, One Shields Drive, Davis, CA 95616, USA.
E-mail: mcheffern@ucdavis.edu

Abstract

Copper is essential in a host of biological processes, and disruption of its homeostasis is associated with diseases including neurodegeneration and metabolic disorders. Extracellular copper shifts in its speciation between healthy and disease states, and identifying molecular components involved in these perturbations could widen the panel of biomarkers for copper status. While there have been exciting advances in approaches for studying the extracellular proteome with mass spectrometry–based methods, the typical workflows disrupt metal–protein interactions due to the lability of these bonds either during sample preparation or in gas-phase environments. We sought to develop and apply a workflow to enrich for and identify protein populations with copper-binding propensities in extracellular fluids using an immobilized metal affinity chromatography (IMAC) resin. The strategy was optimized using human serum to allow for maximum quantity and diversity of protein enrichment. Protein populations could be differentiated based on protein load on the resin, likely on account of differences in abundance and affinity. The enrichment workflow was applied to plasma samples from patients with Wilson's disease and protein IDs and differential abundancies relative to healthy subjects were compared to those yielded from a traditional proteomic workflow. While the IMAC workflow preserved differential abundance and protein ID information from the traditional workflow, it identified several additional proteins being differentially abundant including those involved in lipid metabolism, immune system, and antioxidant pathways. Our results suggest the potential for this IMAC workflow to identify new proteins as potential biomarkers in copper-associated disease states.

Graphical abstract

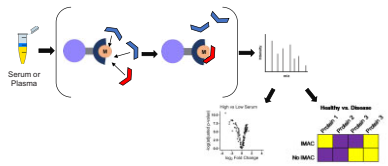

IMAC based workflows reveal differences in protein populations retained on Cu^{2+}–IDA–IMAC resin for both high and low serum loading and when comparing Wilson disease plasma to healthy controls.

Introduction

Copper is an essential metal in biology in processes that include growth, cellular respiration, redox homeostasis, and lipid metabolism.[1–5] While most well studied as a redox-active cofactor tightly bound in enzyme active sites, emerging tools for capturing copper dynamics have illuminated new roles for exchangeable copper pools at protein surfaces in cellular signaling and allosteric regulation, but the majority of the studies on these copper pools have focused on intracellular environments.[4] The extracellular copper pool has received less attention in large part due to a lack of tools for studying this milieu. Traditional, noninvasive methods for assessing extracellular copper parameters rely on quantitation of either total serum/plasma copper with methods such as inductively coupled plasma–mass spectrometry (MS) or measuring the copper-carrying protein, ceruloplasmin (CP), with immunoassays like ELISA. However, the aberrant compartmentalization of extracellular copper pools has been implicated in various disease processes, such as in promoting the aggregation of amyloid-beta peptides in Alzheimer's disease and angiogenesis in cancer progression.[6] In Wilson's disease (WD), which is caused by a mutation of the copper transporter ATP7B, an elevated amount of non-CP-bound copper is observed, but the composition of the ligands for this extracellular copper pool remains unclear.[7,8] Elucidating extracellular components associated with copper under both healthy and disease states may expand our mechanistic understanding of extracellular copper signaling as well as contribute to the pool of potential biomarkers that report on copper status.

Advances in MS-based protein identification have significantly expanded our understanding of the blood proteome.[9,10] However,

Received: May 26, 2022. **Accepted:** July 20, 2022

information on exchangeable metal sites are typically lost in these strategies due to the labile nature of coordination bonds and the redox susceptibility of metals like copper in standard sample preparation workflows do not consider the labile nature of metal-mediated ternary complexes that may have physiological relevance. Additionally, many metal-binding sites are present in low abundance and can frequently evade identification in post-acquisition analytics. In this work, we sought to establish an approach that could preserve and enrich for metal-binding information in plasma and serum samples with subsequent integration into MS-based proteomics workflows.

Immobilized metal affinity chromatography (IMAC) is a powerful chromatographic technique used to enrich analytes with a propensity for metal coordination. Designed in the 1970s, it was optimized for and is most commonly used as a fast and efficient chromatographic method to purify recombinant affinity-tagged (i.e His-tag) proteins.[11] IMAC includes three main components: a solid support bead usually composed of agarose, an extending linker, and a chelate loaded with the metal ion of interest (most commonly Ni^{2+} for His-tagged protein purification). Upon addition of a metal-coordinating species, ternary complex formation occurs between the immobilized metal chelate and the metal-binding species, resulting in retention of the species on the stationary phase, separating it from noncoordinating species in the mobile phase. Bound species can subsequently be eluted by weakening the coordination bond via ligand competition or pH modulation. IMAC has been applied to study endogenous metal coordinating species in a variety of systems, such as rice roots, bacteria, hepatocytes, and serum.[12–15]

In this work, we optimized and applied the IMAC technology alongside gel electrophoresis and MS analysis to enrich for protein populations with Cu^{2+}-binding propensities as a potential approach for assessing copper status. We employed the resin in the form of a solid-phase extraction set up rather than a column format to allow increased residence time of proteins with the resin for maximum protein enrichment. In establishing a workflow, we observed that the composition of the enriched protein population showed key differences between low and high protein loading, offering the possibility of differentiating protein populations based on their Cu^{2+} affinities. We extended our approach to assess retained protein populations in samples acquired from WD patients, and compared the protein identifications to those from a traditional serum proteomic workflow. The IMAC-enriched samples both preserved the changes observed in the traditional workflow as well as identified differentially abundant proteins that did not appear in the traditional workflow. Our results illustrate the utility of Cu^{2+}–IMAC to enrich for copper-interacting protein markers that may otherwise evade identification by current serum and plasma proteomics approaches.

Methods

Cu^{2+}–iminodiacetic acid–IMAC workflow

Cu^{2+}–iminodiacetic acid–IMAC enrichment of pooled human serum proteins

A total of 0.25 mL of iminodiacetic acid (IDA)–IMAC (BioRad) resin was placed in a fritted centrifuge tube, washed with 5 mL of nanopure water, loaded with 1 mL of 0.5 M $CuSO_4$, washed with 5 mL nanopure water to remove unbound Cu^{2+}, equilibrated with 3 mL of loading buffer [phosphate buffered saline (PBS) or bis-tris buffered saline (BTS)], then incubated with various percentages of pooled human serum (Sigma Aldrich) diluted to 500 µL with loading buffer (50, 75, 125, 250, 300 µL of serum corresponding to 10%, 15%, 25%, 50%, and 60% serum, respectively). The proteins were incubated with the Cu^{2+}–IDA–IMAC resin by slowly rotating for 0, 5, 30, and 60 min. Unbound species were washed out with 10 mL wash buffer (PBS or BTS); a final wash of 0.5 mL was collected separately. Retained proteins were then eluted with four 0.5 mL additions of 50 mM ethylenediaminetetraacetic acid (EDTA) dissolved in water and pH adjusted to ~8 with HCl. The protein concentration of each fraction was determined by the Bradford method. For imidazole competition experiments, imidazole was added to 75 µL of pooled human serum diluted to 500 µL in PBS to reach a final concentration of 1, 5, 10, and 20 mM imidazole and incubated for 60 min before washing and eluting with EDTA as described previously. For the unloaded IDA–IMAC experiments, the same procedure was followed with 30% serum being used for protein loading.

Cu^{2+}–IDA–IMAC enrichment of plasma samples from healthy and WD subjects

Human plasma samples from healthy individuals (biological replicates, $n = 4$) and individuals with WD (biological replicates, $n = 4$) were obtained by Dr. Valentina Medici (UC Davis). All subjects provided written informed consent prior to participation following the Declaration of Helsinki. The protocol was approved by UCD Institutional Review Board (protocol # 818454). A total of 75 µL of each sample was diluted to 500 µL in PBS and the IMAC-enrichment procedure was carried out as described earlier with an incubation time of 60 min.

Gel electrophoresis

A total of 12.5 μg of protein from the elution fractions was prepared with 2-mecaptoethanol and lithium dodecyl sulfate (LDS) sample buffer and heated at 70°C for 15 min before loading into a 4-12% Bis-Tris SDS-PAGE gel and run at 100 V for 60 min. After separation, the gel was stained with Imperial protein stain (Pierce) and subsequent destaining with water.

Liquid chromatography–tandem MS analysis of IMAC elution fractions and serum proteins

S-trap protein digestion of serum and plasma samples

An aliquot of the elution fractions from the IMAC experiments corresponding to 300 µg protein (quantified by the Bradford assay) were concentrated on a 3 kDa MWCO filter (MilliporeSigma™ Amicon™ Ultra) and washed with PBS to remove EDTA. The concentrated proteins were then digested following the S-trap procedure (ProtiFi). In brief, equal volume of 100 mM triethyl ammonium bicarbonate (TEAB) with 10% SDS was added to the concentrated protein samples in equal volume, reduced with 5 mM dithiothreitol for 15 min at 55°C, alkylated with 20 mM iodoacetamide for 30 min at room temperature in the dark, then acidified with H_3PO_4 to 1.2%. To the resulting protein solution, six volumes of 90:10 MeOH/1 M TEAB (100 mM final TEAB concentration) was added and inverted immediately. Following colloidal formation, the samples were added to the S-trap, spun at 4000 rpm, and washed with 90:10 MeOH/TEAB solution. The trapped proteins were then digested with 125 µL of 50 mM TEAB containing 10 µg of trypsin overnight at 37°C. After overnight digestion, 125 µL of 50 mM TEAB was added and incubated at 37°C for an additional hour. The tryptic peptides were then eluted with TEAB, 0.1% formic acid (FA), and 50% ACN/0.1% FA and dried via vacuum centrifugation. The traditional workflow followed the

same procedure described earlier without the IMAC enrichment and the MWCO step.

MicroLC–MS/MS analysis

Dried peptides were reconstituted in 0.1% FA and quantified via a peptide fluorescent assay (Pierce). Peptide concentrations were normalized to the lowest sample concentration. A total of 10 µg of peptide were analysed by microflow liquid chromatography connected online to the mass spectrometer (Ultimate 3000 and Orbitrap-HF). Peptides were loaded onto a 1 × 150 mm PepMap C18 column and separated at a flow rate of 50 µL/min with a gradient ranging from 3% acetonitrile to 50% acetonitrile over 50 min, a ramp to 95% for 5 min, followed by a ramp down to 1% over 5 min, followed by a hold at 1% for 5 min. MS1 and MS2 data were acquired on Xcalibur (Thermo Fisher Scientific). MS spray voltage was set to 4 kV; capillary temperature set to 320°C; sheath, auxiliary, and spare gas maintained at 35, 5, and 0, respectively; and S-Lens set to 40. MS1 spectra were collected at a resolution of 60 000 with a automatic gain control (AGC) target of 3e6 and a max ion injection time of 50 ms. The mass range of MS1 was 360–1300 Da. MS2 spectra were collected in using data-dependent acquisition with the top 12 ions from the MS1 scan being selected for fragmentation with dynamic exclusion set to 15 s. The normalized collision energy was set to 28%. For MS2 spectra, the AGC was set to 1e5 with a maximum ion injection time of 86 ms and spectra were acquired at a resolution of 15 000.

Peptide and protein identification and quantification

Raw LC–MS/MS files were searched using MSFragger in FragPipe.[16,17] Spectra were searched against the Uniprot protein database ("homo sapiens") concatenated with the reverse protein sequences (decoys) and common contaminates. A "closed" search was conducted with a precursor tolerance set to −50 and 50 ppm and fragment mass tolerance set to 20 ppm. The search was constrained to semi tryptic enzymatic cleavage with a maximum of two missed cleavages with cysteine alkylation (+57.021460) set as a fixed modification and methione oxidation (+15.994900), pyro-glutamic acid or loss of ammonia at the peptide N-terminus (−17.0265), and loss of water on glutamate on peptide N-terminus (−18.0106) as variable modifications. The reverse-decoy method was used to estimate false discovery rate (FDR). Peptide and protein FDR was set to 0.01. Label free quantification was conducted using the MaxLFQ algorithm employing "match between runs (MBR)" and "normalization of ions" between experiment groups.[18] A minimum of two ions were required for protein quantification and a retention time tolerance of 1 min was used for both feature detection and MBR.

Differential protein abundance detection

Data analysis was conducted in R. The output table containing the protein abundance values ("unique MaxLFQ intensity") produced by MaxLFQ with MBR was used for differential protein abundance determination. Proteins that contained only one unique peptide and contained missing values in any condition were removed. The remaining proteins were median normalized and the *P*-value was calculated using the "moderated *t*-statistic" in the LIMMA R package. The *P*-value was adjusted with Benjamini–Hochberg FDR method. Proteins showing a $\log_2$ fold change ($\log_2$FC) of ±0.75 and adjusted *P*-value less than 0.1 were considered differentially abundant.

Results and discussion

Influence of buffer, serum loading, and incubation time on the amount of protein retained in Cu^{2+}–IMAC resin

The majority of existing protocols for using IMAC resins have been designed and optimized for the purification and isolation of histidine-tag-labeled proteins on Ni^{2+}-loaded columns. We sought to establish a protocol that would allow for us to adapt the method to capture a mixture of unlabeled native species based on their Cu^{2+}-binding affinities. Our initial goal was to select a system that could enrich for a high diversity of proteins with metal-binding capacity while maintaining the protein's native structure, as well as ensure adequate total protein recovery for subsequent analysis. The most common commercially available IMAC resin employ tridentate IDA, tetradentate nitriloacetic acid (NTA), and pentadentate tris-carboxymethyl ethylene diamine (TED) chelates. We reasoned that lower coordinative Cu^{2+} saturation of IDA would allow for greater diversity in protein binding over the NTA and TED chelates, and thus opted to use the commercially available Profinity IDA–IMAC resin (Biorad, Hercules, CA, USA). Instead of using the resin within a continuous-flow column set up, we incorporated an incubation period with the IDA–IMAC to allow flexibility in the adsorption time of the sample to maximize protein capture. In our workflow, the IMAC resin is loaded with Cu^{2+}, washed with water to remove unbound Cu^{2+}, and equilibrated with binding buffer (PBS or BTS). The sample is then introduced to the equilibrated column and the suspension is incubated to allow for protein binding. After incubation the unbound proteins are washed off using binding buffer and retained proteins are eluted with 50 mM EDTA. We first assessed whether this described set up could exhibit a concentration-dependent capture of proteins from human serum. Commercially obtained pooled human serum was diluted in buffer at a fixed volume of 0.5 mL but with varying percentages of serum (50, 75, 125, 200, and 300 μL, corresponding to 10%, 15%, 25%, 40%, and 60% v/v, respectively) and applied to a fixed amount of resin (0.25 mL). We compared two dilution buffers: PBS and Bis-Tris-buffered saline, two common buffers used to maintain physiological pH. Protein was subsequently eluted from the resin with 50 mM EDTA, and total protein levels in the eluents were quantified with a Bradford assay. For both PBS and BTS, a positive linear trend from 10% serum to 40% serum was observed with respect to protein concentration (Fig. 1A). At greater than 40% serum, a break from linearity and a concentration plateau emerged, indicative of protein saturation of the resin above this serum content. The incubations in PBS resulted higher protein recovery than BTS at all volumes tested (Fig. 1A). Since using PBS as the diluent resulted in a higher total protein binding to the resin, we used PBS in subsequent experiments. To assess the effect of incubation time on protein recovery, a 0.5 mL solution of 15% serum in PBS was incubated with 0.25 mL of Cu^{2+}–IDA–IMAC resin at various incubation times. An increase in protein recovery was observed between 0 and 5 min incubation, followed by plateau in protein concentration after 5 min, suggesting that while protein adsorption occurs rapidly, the solid-phase extraction set up allows higher protein recovery than a column chromatography set up, the latter being akin to the 0 min incubation period. Subsequent studies were performed at 60 min incubation times to ensure ample adsorption time onto the resin.

Cu^{2+}–IDA–IMAC protein population dependence

With a protocol established for protein enrichment, we assessed the composition of proteins retained on resin. Serum was applied

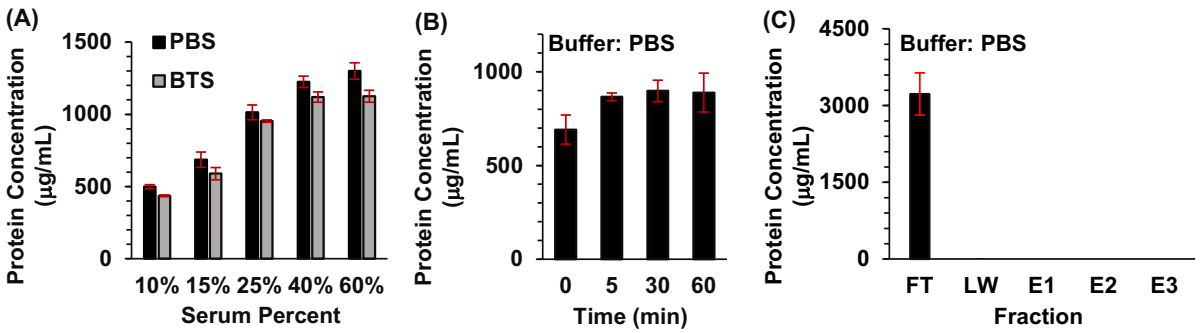

Fig. 1 Protein concentrations of the elution fraction from Cu^{2+}–IDA–IMAC experiments determined by the Bradford assay as a factor of (A) increasing serum percentage (10–60%) and (B) varying incubation time (0–60 min). (C) Protein concentration of the fraction from unloaded IDA–IMAC incubated with 30% serum. Bar plots show mean values with error bars representing standard deviation ($n = 3$). Black bars representing experiments conducted in PBS and gray bars BTS.

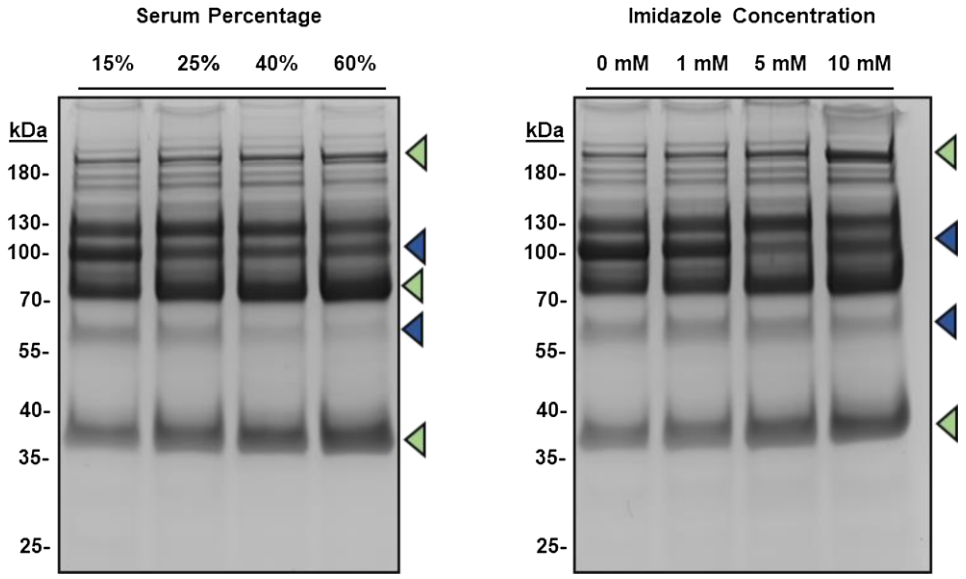

Fig. 2 1D gel electrophoresis of proteins retained and eluted from the Cu^{2+} –IDA–IMAC resin under (left) increasing percentages of pooled human serum (15–60%) and (right) increasing addition of imidazole to the sample prior to loading. Samples were incubated with the resin for 60 min with PBS as the diluent.

to the resin at different serum percentages in PBS for 60 min, and proteins in the elution fractions were separated and stained via 1D gel electrophoresis. The band profiles were compared to assess relative protein populations. Interestingly, the band profile between 55 and 100 kDa shows clear differences at the different serum percentages, indicating that the protein composition is dependent on the total amount of serum applied to the Cu^{2+}–IDA–IMAC resin. For instance, bands at >180 kDa, one at ~70 kDa, and one between ~40 kDa (indicated with green arrows in Fig. 2A) all increase with increasing serum percentage. However, this increase is not global as bands at ~100 and ~60 kDa (indicated with blue arrows in Fig. 2A) decrease with increasing serum percentage. We reasoned that the differential enrichment with respect to serum volume is attributed to the presence of protein competition for the immobilized Cu^{2+}. At low serum volumes, there is an excess of available binding sites on the Cu^{2+}–IDA–IMAC resin. The excess in binding sites may allow for the retention of proteins with a range of binding affinities. Conversely, high serum volumes, corresponding to a higher amount of total protein may lead to a stoichiometric excess of protein with copper-binding ability relative to available coordination sites. In this scenario, proteins with a greater affinity for the immobilized copper ion would outcompete lower-affinity proteins. This hypothesis was first postulated by Porath and Olin where they observed a disproportionate increase in adsorbed protein with increasing serum amount applied to a Ni^{2+} TED column.[19]

To further substantiate this hypothesis, we added increasing amounts of imidazole (final concentration of 0, 1, 5, 10, and 20 mM) to 0.5 mL of a serum solution containing 75 μL serum. Imidazole is able to coordinate to the copper center in Cu^{2+}–IDA with high affinity, thus serving as a model for a high-affinity protein binder.[20,21] Increasing the imidazole content yields a band pattern that resembles the changes observed by increasing serum volume, with similar bands increasing and decreasing accordingly (Fig. 2B). Thus, the changes accompanying increasing imidazole content suggest that on-column competition for the immobilized Cu^{2+} may indeed be what drives differential retention with protein loading. These data suggest serum loading may be potentially leveraged as a means of differentially enriching protein populations based on resin affinity.

Having observed population differences by gel electrophoresis, we aimed to identify the composition of the retained protein pop-

Table 1. List of differentially abundant proteins from serum loading experiments[a]

Protein name	Absolute log_2 fold change	Adjusted *P*-value (FDR)
Proteins more abundant at higher serum percentage		
Alpha-2-HS-glycoprotein (AHSG)	0.88	1.53E-07
Coagulation factor XII (F12)	1.08	5.15E-07
Coagulation factor V (F5)	0.91	9.37E-06
Complement C1q subcomponent subunit A (C1QA)	0.85	3.41E-07
Complement C1q subcomponent subunit B (C1QB)	0.90	5.39E-06
Complement C1q subcomponent subunit C (C1QC)	0.80	1.69E-05
Complement component (C6)	0.90	2.37E-06
Complement factor H (CFH)	0.94	1.55E-07
Hemopexin (HPX)	0.84	2.03E-07
Histidine-rich glycoprotein (HRG)	0.91	1.24E-06
Proteins more abundant at lower serum percentage		
Albumin (HSA)	1.89	6.05E-06
Ceruloplasmin (CP)	1.26	2.35E-08
Complement component (C2)	0.89	1.47E-03
Complement component (C9)	2.47	1.24E-08
Complement factor B (CFB)	0.90	4.90E-07

[a]Magnitude of change between conditions are represented as absolute value of log_2 fold change over the contrasting condition.

ulation under high and low serum percentages. A total of 15% and 60% serum in a fixed volume of 0.5 mL in PBS were used as "low" and "high" serum amount, respectively. Each condition was run on the IMAC resin in quadruplicate and the eluents were analysed by microLC–tandem MS (μLC–MS/MS) coupled with a protein identification via MSFragger. The workflow identified more than 200 (Supplementary Table S1) proteins filtered at a 99% protein probability with a minimum of two peptides per ID. Differential binding between high and low serum percentages was assessed by filtering out proteins with any missing values, quantile normalizing the protein intensity values, applying LIMMA to generate a moderated *t*-statistic and subsequent *P*-value. The *P*-values were adjusted via the Benjamini–Hochberg method to adjust for multiple hypothesis testing. Proteins that showed ±0.75 log_2FC and FDR adjusted *P*-value of less than 0.1 were considered differentially abundant indicating differential binding with respect to serum volume (Table 1).

The differential-binding analysis revealed serum proteins with elevated enrichment in the high serum samples with previous associations with copper. For instance, hemopexin (HPX) showed elevated enrichment in the high serum samples. HPX is an acute phase serum protein expressed by the liver that binds to heme with a strong affinity (K_d < 1 pM).[22] The main role of HPX is to participate in heme recycling by binding and transporting to the LDL-receptor-related 1 protein for internalization.[23] Previous research indicates HPX's ability to bind divalent metals, such as Cu^{2+}.[24] The endocytosis of the heme-HPX complex increases cytosolic copper, while metal binding leads to a decrease in the heme-HPX complex stability.[25] Another example of a protein with elevated enrichment in the high serum samples is coagulation factor XII (F12); a previous study has shown that metal ions, including copper, may indeed activate F12-mediated coagulation.[26] Finally, peptide fragments of another identification, histidine-rich glycoprotein (HRG), have been shown to bind copper, and copper has been proposed to be associated with the antiangiogenic activity of the protein.[27,28]

Other proteins with elevated enrichment in the high serum samples include proteins associated with metabolic disorders in which copper misregulation has been implicated. Of note is alpha-2-HS-glycoprotein (AHSG), also referred to as fetuin-A (Fet-A), a glycoprotein synthesized in the liver involved in various processes including inhibition of ectopic calcification and fatty acid metabolism.[29] Moreover, elevated Fet-A has been associated with metabolic disorders including nonalcoholic fatty liver, type 2 diabetes, and metabolic syndrome, all of which present altered copper homeostasis.[30]

The abundance of various members of the complement system is also dependent on the amount of serum applied. CFH, C1QA, C1QB, C1QC, and C6 were higher in abundance in the high serum experiment while CFB, C2, and C9 were higher in the low serum experiment. The association of complement factor H (CFH) with copper has been observed within the context of inducing CFH oligomerization.[31] These findings are interesting as the complement system is involved in immune system response to infections and an increase in copper levels has been observed at sites of infection.[32,33] The exact biological ramifications of copper accumulation at these sites are currently unknown. However, our experiments may offer the speculation toward dynamic differential copper binding directly to proteins of the complement system within these sites.

At higher serum volume, CP is inversely correlated with factor V (F5) and factor XII, with CP being less enriched and the latter two showing increased enrichment. The opposite binding trend for CP and F5 is intriguing as both have been considered members of the same protein family and evolutionary linked.[34] While CP has been more extensively studied for its role in copper metabolism and transport, F5 has been suggested to bind copper in a 1:1 metal–protein ratio.[35] A study conducted with metals, including Cu^{2+}, immobilized on NTA-bound liposomes induced clotting at a higher rate than without the metals present.[26] This observation was attributed to an interaction between the immobilized metals and various contact pathway proteins. Along with the observed elevated enrichment of F12 in the high serum samples, our experiments may suggest possible metal/protein interactions in influencing contact pathway activation.

Unexpectedly, serum albumin showed a decrease in abundance with respect to increasing serum applied to the Cu^{2+}–IDA–IMAC resin. Albumin is a highly abundant serum protein containing multiple metal-binding sites including a Cys34, an N-terminal binding site (NBS), a multi-metal binding site (MBS), and an unknown fourth site. The NBS site (Asp–Ala–His) has an estimated

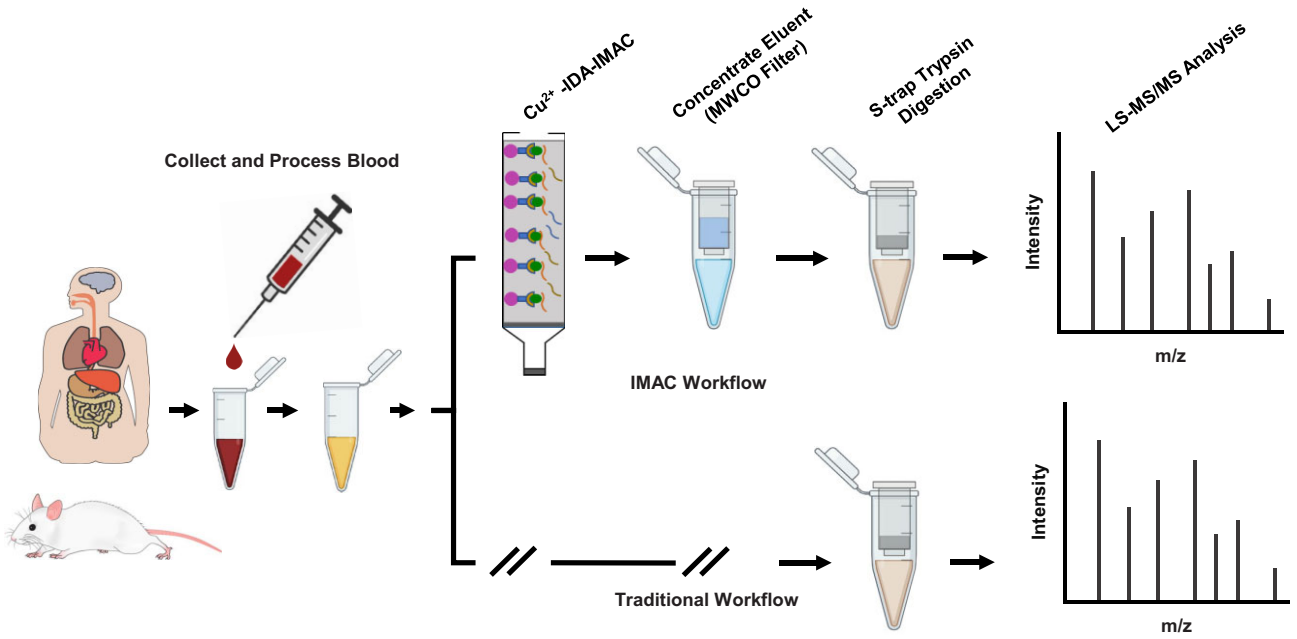

Fig. 3 Contrast between IMAC workflow and traditional workflow. In the IMAC workflow, blood is collected and processes into plasma or serum followed by application of Cu^{2+}–IMAC and a desalting step with a 3 kDa MWCO filter. Post desalting, proteins are digested via a modified S-trap (ProtiFi) procedure, analysed via microflowLC–MS/MS, identified by MSFragger, and differential abundance is processed via LIMMA. Traditional workflows include all steps except the IMAC enrichment and desalting steps. Created with BioRender.com.

dissociation constant between $\log K_d = -11.18$ and $\log K_d = -16.18$ and transports copper in the bloodstream.[36] However, despite the high Cu^{2+} affinity of the NBS site, it is unknown if albumin is binding to the immobilized copper at the NBS site. If binding occurs at the NBS site, the formation of the tertiary complex between the Cu^{2+}–IDA–IMAC resin and albumin may lead to significant reduction in binding strength due to the incomplete ATCUN–Cu^{2+} complex formation, preventing one or more coordinating sites from interacting with the immobilized Cu^{2+}. If the geometry of albumin binding is altered, then the actual binding strength may be lowered resulting in displacement by other proteins at higher serum volumes. This supports our hypothesis that the application and comparison of varying serum percentages to the IMAC resin can be used to gauge the strength of ternary complex formation of serum proteins.

Prior studies have determined that IMAC resins can capture proteins that may not natively bind copper, but have copper-binding propensities through features such as surface-exposed histidines.[37] Our studies illustrate that in addition to surface accessibility, sample loading may add another layer of selection for protein populations based on their affinities for the copper chelate. To date no detailed and in-depth proteomic analysis of the protein population changes with respect to the total protein applied on an IMAC resin have been reported. While further focused studies are required to understand the dynamic nature of metal–protein binding and both the specifics and detailed thermodynamics of the protein identified, our studies demonstrate the potential for IMAC as a tool to gauge the relative strength of Cu^{2+} binding of species present in a complex biological matrix such as serum. Furthermore, our studies demonstrate that the inclusion of an IMAC-enrichment step can reduce the complexity of a clinical sample to allow for the retained population to be leveraged for assessing physiological metal status.

Protein population is different with IMAC enrichment–Wilson's disease

Having established the abilities of our Cu^{2+}–IDA–IMAC-based protocol to enrich for specific populations with sufficient protein abundance and diversity, as well as differentiate populations based on the amount of serum loaded, we tested the utility of our approach in extracting potentially unique diagnostic information associated with WD. As patients with WD exhibit impairments in CP loading, it is posited that these results in a higher level of non-CP-bound copper in the blood; yet it remains uncertain whether any changes occur on the composition of copper-binding species. We analysed plasma samples from healthy controls (CTL, $n = 4$) and WD ($n = 4$) patients by both the IMAC workflow and a traditional proteomics workflow (Fig. 3). Over 200 proteins were identified by both workflows (Supplementary Tables S2 and S3) with a less than 1% FDR. To assess the differences between the traditional workflow and IMAC workflow, the data were divided into two subgroups: Unique MaxLFQ intensity value from proteins with no missing values, and those where there were at most one missing value in a condition and none in the other. For the proteins with no missing values, differential abundance analysis was carried out as previously described. In the latter scenario, we assumed the protein was either not present or below the detection limit.

In comparing abundancies between CTL and WD samples, the traditional workflow produced eight differentially abundant proteins while the IMAC workflow produced 36 (Fig. 4A–C), indicating that IMAC may allow for enrichment of a protein population that is otherwise missed in the absence of this step. Several proteins, including alpha-2-macroglobin, CP, complement component C7 (C7), apolipoprotein L1 (APOL1), and amyloid P-component were found to be differentially abundant in WD plasma in both workflows. In addition to differential abundances in proteins between CTL and WD samples, in analysing the collective identifications

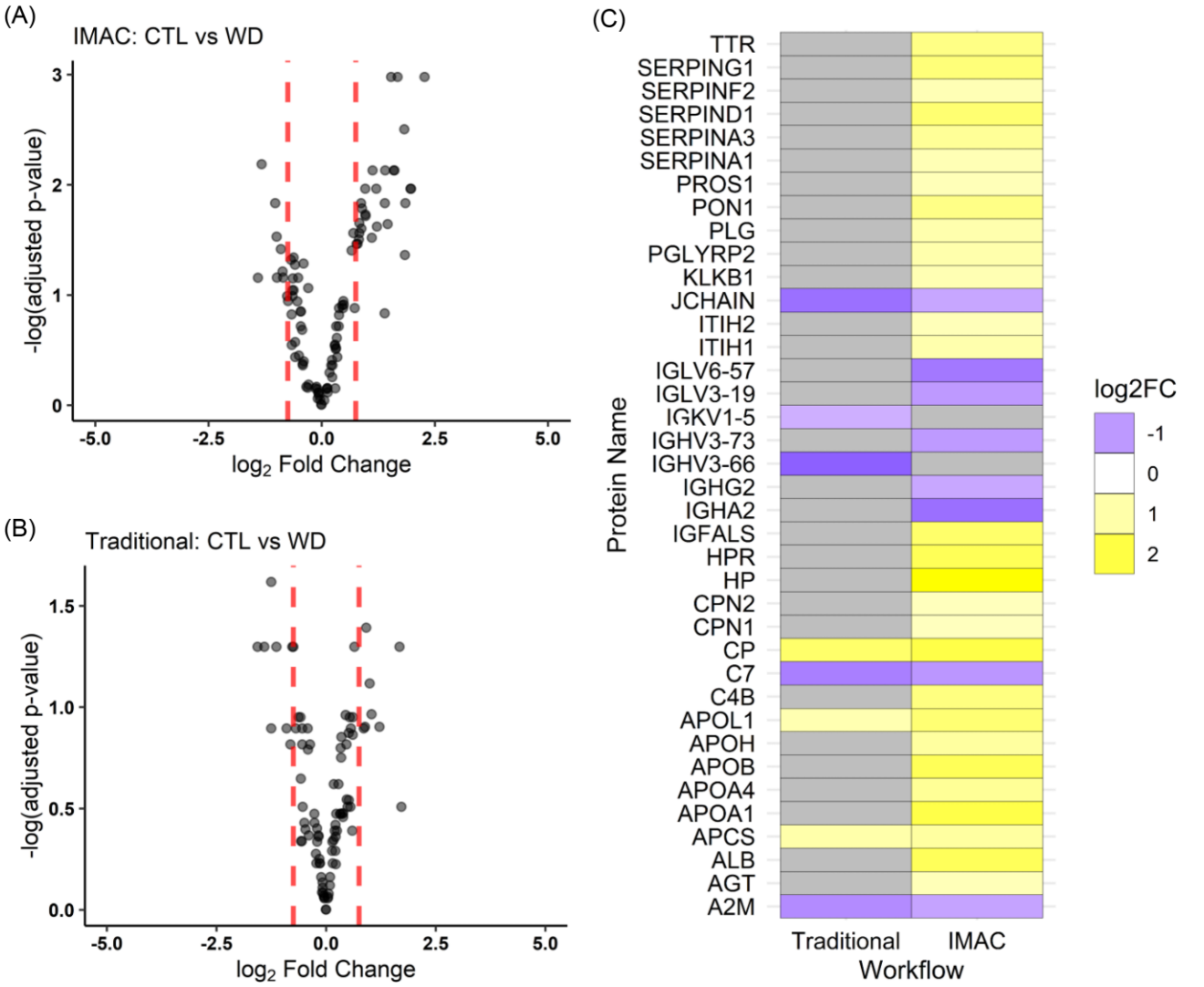

Fig. 4 Volcano plots (−$\log_{10}$ of adjusted *P*-value[Q-value] versus $\log_2$FC) of each contrast made. (A) IMAC: Healthy control (CTL) versus WD (B) traditional: Healthy controls (CTL) versus WD. Vertical dashed lines represent logFC change cutoffs at −0.75 and 0.75. Negative $\log_2$ fold changes in A and B indicate proteins were less abundant in healthy than WD plasma. (C) Heatmap of differentially abundant proteins found in the traditional and IMAC workflows. Blue indicates proteins found more abundant in the WD plasma. Yellow indicates proteins found less abundant in WD plasma. Gray indicates proteins not found differentially abundant.

made across both CTL and WD samples, we identified that the IMAC procedure enriched for seven proteins that were otherwise below detection via the traditional workflow. Conversely, three proteins were identified with the traditional workflow, which were excluded from detection in the IMAC-enriched samples (Supplementary Table S4).

In both the traditional and IMAC workflows, various apolipoproteins (designated with the APO prefix) were observed to be differentially abundant. Apolipoproteins are mainly synthesized in the liver and intestines, and participate in triglyceride and cholesterol transport.[38] Apolipoproteins are potentially connected to WD in that aberrant cholesterol, very-low-density lipoprotein, and lipid metabolism have been observed in patients as well as in *Atp7b*$^{-/-}$ knockout mice, model of WD.[39,40] In the traditional workflow, APOL1 showed a decrease in abundance in WD plasma. In contrast, the IMAC workflow showed a decrease in both APOL1 and APOC1 alongside the decreased abundance of additional apolipoproteins, APOA1, APOA4, APOB, and APOH (beta-2-glycoprotein), compared to healthy controls. Furthermore, APOF was detected in CTL samples but not detected in WD plasma in both the traditional and IMAC workflows. Apolipoproteins have been previously associated with hepatic injury. For instance, a previous proteomics found a decrease in APOE and APOL1 in the plasma of patients with different stages of liver fibrosis due to chronic hepatitis C.[41] Additionally, changes to apolipoproteins have been loosely associated with copper. For instance, an inverse correlation was observed between copper and apolipoproteins, with elevated APOA1, APOA2, and APOE identified in rats with copper deficiency.[42] Copper has also been shown to bind to and be reduced by APOB within the context of LDL oxidation.[43] Moreover, certain lipoproteins have been suggested to utilize copper for ferroxidase activity, such as the >800 kDa protein "ferroxidase II."[44,45] While many questions remain regarding how apolipoprotein and lipoprotein, serum copper, and hepatic metabolism are interconnected, our studies alongside the previous studies may highlight their interplay as potential markers in diseases such as WD.

Several proteins were determined to be differentially abundant uniquely in the IMAC workflow, such as transthyrien (TTR), haptoglobin, and paraoxonase/arylesterase 1 (PON1). Several studies have pointed to conformational changes to TTR in the presence of several metals, with metals mediating potential enzymatic function as well as even neuroprotective roles such as amyloid-beta binding.[46–49] Haptoglobin's primary role is to bind to free hemoglobin leading to the clearance and degradation of hemoglobin and a decrease in haptoglobin is often associated with hemolytic anemia, which results from the lysing of red blood cells.[50,51] Hemolytic anemia is a common presentation of WD with approximately 10–15% of WD patients developing the complication. PON1 has been shown to potentiate CCl_4 liver damage in mice transfected with human PON1, suggesting a protective function against oxidative damage.[52] These data suggest retention of biologically relevant trends as there is precedence of the aforementioned proteins being differentially abundant in WD.[53]

Interestingly, sulfhydryl oxidase 1 (QSOX1) was identified exclusively in the IMAC workflow. QSOX1 is involved in disulfide bond formation and positively correlated with pancreatic and breast tumor cell growth.[54] QSOX1 may act in a protective manner during periods of increased oxidative stress, as observed in in PC12 and overexpression studies with the breast cancer cell line MCF-7.[55] To date, no correlation between QSOX1 or Cu^{2+} binding has been observed, although an increase in both extracellular non-CP-bound copper and oxidative stress has been documented in WD. The mechanism of QSOX1 in protecting against oxidative stress remains elusive and further investigation is necessary to support a relation between copper, QSOX1, and WD. However, it may be possible for QSOX1 to bind directly to non-CP-bound copper in the extracellular space and reduce the ability for reactive oxygen species (ROS) generation. Additionally, the IMAC workflow revealed beta-Ala-His peptidase (CNDP1) to be present only in the healthy plasma samples. CNDP1 acts to degrade the dipeptide B-Ala-His (carnosine), which has been associated with protection against reactive species generation and has been suggested to be directly involved in maintaining copper homeostasis.[56,57] CNDP1 knockout studies lead to an increase in carnosine levels and our data imply that CNDP1 levels are lower in WD, which could be linked to a systemic reaction to increased oxidative stress by excess copper in the blood. Taken together, these two protein hits demonstrate the potential value of the IMAC workflow for enriching otherwise overlooked proteins with implications in both disease pathology as well as in biomarker discovery.

A common concern with enrichment techniques is the added variability they may impart. For each additive step in a workflow, artificial variability is added onto already complex biological variability that confounds data and ultimately reduces significant conclusions. In our results, both the protein identifications as well as the patterns of differential abundance with WD follow the same trends in both workflows. This indicates that the IMAC workflow does not occlude information obtained in the traditional workflow. Importantly, while preserving biological trends in the traditional workflow, the addition of IMAC also brings to light proteins that are otherwise absent in the traditional workflow (QSOX1 and CNDP1) with potential disease relevance.

We posit that the difference in protein population profiles observed in the IMAC flow compared to the traditional IMAC workflow when contrasting healthy and WD plasma may be due to ligands comprising the non-CP-bound copper known to be present in WD. While the exact concentration of cheatable metal micronutrients in the blood is poorly understood, it is well established that the amount of chelatable copper increases in WD. The increase in chelatable copper could shift the balance of metalated serum proteins, which in turn would influence the ability of such proteins to bind to the Cu^{2+} loaded IMAC resin. For example, if in a WD sample, a given protein is occupied with non-CP-bound copper that is otherwise vacant in a healthy sample, this may preclude the ability of that protein to bind the Cu^{2+} loaded IMAC resin, manifesting as a loss of that protein in the IMAC-retained population. Alternatively, copper occupation could shift the binding interaction between the protein and IMAC resin to more accessible site, possibly lowering enrichment efficacy. In either case, shifts in IMAC-enriched population may offer valuable information in tandem with other clinical parameters for improving the comprehensiveness of copper status assessment.

Conclusion

Copper is essential for maintaining biological homeostasis and must be tightly regulated to preserve proper physiology or risk disease onset. Despite the importance of copper in biological processes, much remains to be understood with respect to the dynamics of copper regulation, particularly in extracellular environments, in part due to the dearth of techniques to study the proteins involved, many of which may have low abundance. To this end, we employed Cu^{2+}–IMAC coupled with a proteomics workflow as a means of enriching for copper-associated parameters. We optimized the conditions for metal-binding protein enrichment on a Cu^{2+}–IDA–IMAC resin via a solid-phase extraction set up that is amenable to high-throughput workflows. We found that distinct protein changes occur with increasing serum volume applied, and attributed these differences to protein competition for the immobilized Cu^{2+}, resulting in an increase of stronger Cu^{2+}-binding proteins at higher volumes, pointing the possibility of using IMAC to differentially enrich for proteins based on their Cu^{2+} affinities. We also contrasted healthy plasma to plasma from patients diagnosed with WD using a proteomics workflow with and without the addition of Cu^{2+}–IMAC. The integration of the IMAC workflow both preserved expected protein differences as well as identified additional differentially abundant proteins when compared to the no-IMAC workflow. The differences in proteins found differentially abundant between both workflows suggest IMAC provides an additional layer of information regarding protein–copper binding or as pseudo-depletion step of highly abundant serum proteins. We note that the proteins identified in the IMAC workflow only inform on a protein population with the propensity for Cu^{2+} binding. Further structural as well as biological studies are required to validate whether the individual proteins are native cuproproteins as well as their viability as biomarkers for copper status across different disease states. Additionally, the current experimental design will exclude proteins that bind Cu^{2+} with high affinities that prevent ligand exchange; however, future work may focus on modulating sample preparation in tandem with IMAC to recover this information. Nevertheless, this work demonstrates the ability of the Cu^{2+} IMAC technique to efficiently assess differences in the global profile of the serum proteome based on their copper affinities and could provide insight into how these modulations influence copper regulation.

Supplementary material

Supplementary data are available at *Metallomics* online.

Acknowledgements

We thank Dr. William Jewell for training and assistance on the Orbitrap HF Mass Spectrometer and the Campus Mass Spectrometry Facility (CMSF) for the use of the instrument. We also thank the reviewers for their helpful feedback and all members of the Heffern lab for valuable discussions.

Author contributions

S.E.J. and M. C. H. designed all experiments. S.E.J, V.A.S, and A.C, performed all experiments and collected data. S.E.J. and M.C.H. analysed the data. V.M. collected and provided the human serum samples. S.E.J organized the manuscript, and S.E.J. and M.C.H. wrote and edited the manuscript with input from V.M. M.C.H. conceived the study and was the major supervisor on overall direction of the study.

Funding

This work was supported by the National Institute of Health (NIH MIRA 5R35GM133684-02 and NIH DK104770) and the National Science Foundation (NSF CAREER 2048265). We also thank the Hartwell Foundation for their generous support for M.C.H. as a Hartwell Individual Biomedical Investigator, as well as the UC Davis CAMPOS Program and the University of California's Presidential Postdoctoral Fellowship Program for their support of M.C.H. as a CAMPOS Faculty Fellow and former UC President's Postdoctoral Fellow, respectively.

Conflicts of interest

The authors have no conflicts of interest to declare.

Data availability statement

The data underlying this article will be shared on reasonable request to the corresponding author.

References

1. M. C. Heffern, H. M. Park, H. Y. Au-Yeung, G. C. Van de Bittner, C. M. Ackerman, A. Stahl and C J. Chang, In vivo bioluminescence imaging reveals copper deficiency in a murine model of nonalcoholic fatty liver disease, *Proc Natl Acad Sci USA*, 2016, 113 (50), 14219–14224.
2. R. A. Festa and D J. Thiele, Copper: an essential metal in biology, *Curr. Biol.*, 2011, 21 (21), R877–R883.
3. J. A. Tainer, E. D. Getzoff, J. S. Richardson and D C. Richardson, Structure and mechanism of copper, zinc superoxide dismutase, *Nature*, 1983, 306 (5940), 284–287.
4. L. Krishnamoorthy, J. A. Cotruvo, J. Chan, H. Kaluarachchi, A. Muchenditsi, V. S. Pendyala, S. Jia, A. T. Aron, C. M. Ackerman, M. N. V. Wal, T. Guan, L. P. Smaga, S. L. Farhi, E. J. New, S. Lutsenko and C J. Chang, Copper regulates cyclic-amp-dependent lipolysis, *Nat. Chem. Biol.*, 2016, 12 (8), 586–592.
5. N. H. O. Harder, H. P. Lee, V. J. Flood, J. A. San Juan, S. K. Gillette and M. C. Heffern, Fatty acid uptake in liver hepatocytes induces relocalization and sequestration of intracellular copper, *Front Mol Biosci*, 2022, 9, 1–13.
6. E D. Harris, A requirement for copper in angiogenesis, *Nutr. Rev.*, 2004, 62 (2), 60–64.
7. C. Gerosa, D. Fanni, T. Congiu, M. Piras, F. Cau, M. Moi and G. Faa, Liver pathology in wilson's disease: from copper overload to cirrhosis, *J. Inorg. Biochem.*, 2019, 193, 106–111.
8. J. J. O'Sullivan, V. Medici and M C. Heffern, A caged imidazopyrazinone for selective bioluminescence detection of labile extracellular copper(II), *Chem. Sci.*, 2022, 13 (15), 4352–4363.
9. P. E. Geyer, L. M. Holdt, D. Teupser and M. Mann, Revisiting biomarker discovery by plasma proteomics, *Mol. Syst. Biol.*, 2017, 13 (9), 942.
10. V. Ignjatovic, P. E. Geyer, K. K. Palaniappan, J. E. Chaaban, G. S. Omenn, M. S. Baker, E. W. Deutsch and J M. Schwenk, Mass spectrometry-based plasma proteomics: considerations from sample collection to achieving translational data, *J. Proteome Res.*, 2019, 18 (12), 4085–4097.
11. J. PORATH, J. A. N. CARLSSON, I. OLSSON and G. BELFRAGE, Metal chelate affinity chromatography, a new approach to protein fractionation, *Nature*, 1975, 258 (5536), 598–599.
12. Y. Song, H. Zhang, C. Chen, G. Wang, K. Zhuang, J. Cui and Z. Shen, Proteomic analysis of copper-binding proteins in excess copper-stressed rice roots by immobilized metal affinity chromatography and two-dimensional electrophoresis, *Biometals*, 2014, 27 (2), 265–276.
13. Y. Wang, C.-N. Tsang, F. Xu, P.-W. Kong, L. Hu, J. Wang, I. K. Chu, H. Li and H. Sun, Bio-coordination of bismuth in *helicobacter pylori* revealed by immobilized metal affinity chromatography, *Chem. Commun.*, 2015, 51 (92), 16479–16482.
14. S. D. Smith, Y. M. She, E. A. Roberts and B. Sarkar, Using immobilized metal affinity chromatography, two-dimensional electrophoresis and mass spectrometry to identify hepatocellular proteins with copper-binding ability, *J. Proteome Res.*, 2004, 3 (4), 834–840.
15. F. Wang, C. Chmil, F. Pierce, K. Ganapathy, B. B. Gump, J. A. MacKenzie, Y. Mechref and K. Bendinskas, Immobilized metal affinity chromatography and human serum proteomics, *J. Chromatogr. B*, 2013, 934, 26–33.
16. A. T. Kong, F. V. Leprevost, D. M. Avtonomov, D. Mellacheruvu and A I. Nesvizhskii, MSFragger: ultrafast and comprehensive peptide identification in mass spectrometry-based proteomics, *Nat. Methods*, 2017, 14 (5), 513–520.
17. F. Yu, G. C. Teo, A. T. Kong, S. E. Haynes, D. M. Avtonomov, D. J. Geiszler and A I. Nesvizhskii, Identification of modified peptides using localization-aware open search, *Nat. Commun.*, 2020, 11 (1), 4065.
18. F. Yu, S. E. Haynes and A I. Nesvizhskii, IonQuant enables accurate and sensitive label-free quantification with FDR-controlled match-between-runs, *Mol. Cell. Proteomics*, 2021, 20, 100077.
19. J. Porath and B. Olin, Immobilized metal affinity adsorption and immobilized metal affinity chromatography of biomaterials. serum protein affinities for gel-immobilized iron and nickel ions, *Biochemistry*, 1983, 22 (7), 1621–1630.
20. J. Porath, Immobilized metal ion affinity chromatography, *Protein Expression Purif.*, 1992, 3 (4), 263–281.
21. J. A. Bornhorst and J J. Falke, Purification of proteins using polyhistidine affinity tags, *Methods Enzymol.*, 2000, 326, 245–254.
22. E. Tolosano and F. Altruda, Hemopexin: structure, function, and regulation, *DNA Cell Biol.*, 2002, 21 (4), 297–306.
23. E. Tolosano, S. Fagoonee, N. Morello, F. Vinchi and V. Fiorito, Heme scavenging and the other facets of hemopexin, *Antioxid. Redox Signaling*, 2009, 12 (2), 305–320.
24. M. R. Mauk, F. I. Rosell, B. Lelj-Garolla, G. R. Moore and A G. Mauk, Metal ion binding to human hemopexin, *Biochemistry*, 2005, 44 (6), 1864–1871.

25. A. Smith, K. R. Rish, R. Lovelace, J. F. Hackney and R M. Helston, Role for copper in the cellular and regulatory effects of heme-hemopexin, *Biometals*, 2009, 22 (3), 421–437.
26. N. J. Mutch, E. K. Waters and J. H. Morrissey, Immobilized transition metal ions stimulate contact activation and drive factor XII-mediated coagulation, *J. Thromb. Haemost.*, 2012, 10 (10), 2108–2115.
27. A. Magrì, G. Grasso, F. Corti, F. Finetti, V. Greco, A. M. Santoro, S. Sciuto, D. La Mendola, L. Morbidelli and E. Rizzarelli, Peptides derived from the histidine-proline rich glycoprotein bind copper ions and exhibit anti-angiogenic properties, *Dalton Trans.*, 2018, 47 (28), 9492–9503.
28. D. La Mendola, A. Magrì, A. M. Santoro, V. G. Nicoletti and E. Rizzarelli, Copper(II) interaction with peptide fragments of histidine-proline-rich glycoprotein: speciation, stability and binding details, *J. Inorg. Biochem.*, 2012, 111, 59–69.
29. W. Jahnen-Dechent, A. Heiss, C. Schäfer, M. Ketteler and D A. Towler, Fetuin-a regulation of calcified matrix metabolism, *Circ. Res.*, 2011, 108 (12), 1494–1509.
30. L. Bourebaba and K. Marycz, Pathophysiological implication of fetuin-a glycoprotein in the development of metabolic disorders: a concise review, *J Clin Med*, 2019, 8 (12), 2033.
31. R. Nan, J. Gor, I. Lengyel and S J. Perkins, Uncontrolled zinc- and copper-induced oligomerisation of the human complement regulator factor H and its possible implications for function and disease, *J. Mol. Biol.*, 2008, 384 (5), 1341–1352.
32. J. V. Sarma and P A. Ward, The complement system, *Cell Tissue Res.*, 2011, 343 (1), 227–235.
33. K. Y. Djoko, C. Y. Ong, M. J. Walker and A G. McEwan, The role of copper and zinc toxicity in innate immune defense against bacterial pathogens, *J. Biol. Chem.*, 2015, 290 (31), 18954–18961.
34. W. R. Church, R. L. Jernigan, J. Toole, R. M. Hewick, J. Knopf, G. J. Knutson, M. E. Nesheim, K. G. Mann and D N. Fass, Coagulation factors V and VIII and ceruloplasmin constitute a family of structurally related proteins, *Proc. Natl. Acad. Sci.*, 1984, 81 (22), 6934 LP–6936937.
35. K. G. Mann, C. M. Lawler, G. A. Vehar and W R. Church, Coagulation factor V contains copper ion, *J. Biol. Chem.*, 1984, 259 (21), 12949–12951.
36. T. Kirsipuu, A. Zadorožnaja, J. Smirnova, M. Friedemann, T. Plitz, V. Tõugu and P. Palumaa, Copper(II)-binding equilibria in human blood, *Sci. Rep.*, 2020, 10 (1), 5686.
37. V. Gaberc-Porekar and V. Menart, Perspectives of immobilized-metal affinity chromatography, *J. Biochem. Bioph. Methods*, 2001, 49 (1-3), 335–360.
38. I. Ramasamy, Recent advances in physiological lipoprotein metabolism, *Clin Chem Lab Med*, 2014, 52 (12), 1695–1727.
39. T. A. Mazi, N. M. Shibata and V. Medici, Lipid and energy metabolism in wilson disease, *Liver Res*, 2020, 4 (1), 5–14.
40. D. Huster, T. D. Purnat, J. L. Burkhead, M. Ralle, O. Fiehn, F. Stuckert, N. E. Olson, D. Teupser and S. Lutsenko, High copper selectively alters lipid metabolism and cell cycle machinery in the mouse model of wilson disease, *J. Biol. Chem.*, 2007, 282 (11), 8343–8355.
41. B. Gangadharan, M. Bapat, J. Rossa, R. Antrobus, D. Chittenden, B. Kampa, E. Barnes, P. Klenerman, R. A. Dwek and N. Zitzmann, Discovery of novel biomarker candidates for liver fibrosis in hepatitis c patients: a preliminary study, *PLoS One*, 2012, 7 (6), e39603–e39603.
42. K Y. Lei, Alterations in plasma lipid, lipoprotein and apolipoprotein concentrations in copper-deficient rats, *J. Nutr.*, 1983, 113 (11), 2178–2183.
43. C. Batthyány, C. X. C. Santos, H. Botti, C. Cerveñansky, R. Radi, O. Augusto and H. Rubbo, Direct evidence for Apo b-100-mediated copper reduction: studies with purified Apo B-100 and detection of tryptophanyl radicals, *Arch. Biochem. Biophys.*, 2000, 384 (2), 335–340.
44. R. W. Topham and E. Frieden, Identification and purification of a non-ceruloplasmin ferroxidase of human serum, *J. Biol. Chem.*, 1970, 245 (24), 6698–6705.
45. A. Garner, L. Tosi and M. Steinbuch, Ferroxidase II. the essential role of copper in enzymatic activity, *Biochem. Biophys. Res. Commun.*, 1981, 98 (1), 66–71.
46. L. Ciccone, N. Tonali, W. Shepard, S. Nencetti and E. Orlandini, Physiological metals can induce conformational changes in transthyretin structure: neuroprotection or misfolding induction? *Crystals*, 2021, 11 (4), 354.
47. R. Costa, F. Ferreira-da-Silva, M. J. Saraiva and I. Cardoso, Transthyretin protects against a-beta peptide toxicity by proteolytic cleavage of the peptide: a mechanism sensitive to the kunitz protease inhibitor, *PLoS One*, 2008, 3 (8), e2899.
48. I. E. Gouvea, M. Y. Kondo, D. M. Assis, F. M. Alves, M. A. Liz, M. A. Juliano and L. Juliano, Studies on the peptidase activity of transthyretin (TTR), *Biochimie*, 2013, 95 (2), 215–223.
49. R. Costa, A. Gonçalves, M. J. Saraiva and I. Cardoso, Transthyretin binding to a-beta peptide – Impact on a-beta fibrillogenesis and toxicity, *FEBS Lett.*, 2008, 582 (6), 936–942.
50. A. W. Y. Shih, A. McFarlane and M. Verhovsek, Haptoglobin testing in hemolysis: measurement and interpretation, *Am. J. Hematol.*, 2014, 89 (4), 443–447.
51. J. Phillips and A C. Henderson, Hemolytic anemia: evaluation and differential diagnosis, *Am. Fam. Physician*, 2018, 98, 354–361.
52. C. Zhang, W. Peng, X. Jiang, B. Chen, J. Zhu, Y. Zang, J. Zhang, T. Zhu and J. Qin, Transgene expression of human PON1 Q in mice protected the liver against CCl4-induced injury, *J. Gene Med.*, 2008, 10 (1), 94–100.
53. M. Lacombe, M. Jaquinod, L. Belmudes, Y. Couté, C. Ramus, F. Combes, T. Burger, E. Mintz, J. Barthelon, V. Leroy, A. Poujois, A. Lachaux, F. Woimant and V. Brun, Comprehensive and comparative exploration of the Atp7b−/− mouse plasma proteome†, *Metallomics*, 2020, 12 (2), 249–258.
54. D. F. Lake and D O. Faigel, The emerging role of QSOX1 in cancer, *Antioxid. Redox Signaling*, 2014, 21 (3), 485–496.
55. C. Morel, P. Adami, J.-F. Musard, D. Duval, J. Radom and M. Jouvenot, Involvement of sulfhydryl oxidase QSOX1 in the protection of cells against oxidative stress-induced apoptosis, *Exp. Cell. Res.*, 2007, 313 (19), 3971–3982.
56. A. Barca, S. Ippati, E. Urso, C. Vetrugno, C. Storelli, M. Maffia, A. Romano and T. Verri, Carnosine modulates the Sp1-Slc31a1/Ctr1 copper-sensing system and influences copper homeostasis in murine cns-derived cells, *Am J Physiol - Cell Physiol*, 2019, 316 (2), C235–C245.
57. N. Arnal, M. J. T. de Alaniz and C A. Marra, Carnosine and neocuproine as neutralizing agents for copper overload-induced damages in cultured human cells, *Chem. Biol. Interact.*, 2011, 192 (3), 257–263.